JP3J.5 **RADAR OBSERVATIONS DURING NAME 2004**
PART I: DATA PRODUCTS AND QUALITY CONTROL

Timothy J. Lang*, Rob Cifelli, Lee Nelson, Stephen W. Nesbitt,
Gustavo Pereira, and Steven A. Rutledge
Colorado State University, Fort Collins, Colorado

David Ahijevych and Rit Carbone
National Center for Atmospheric Research, Boulder, Colorado

1. INTRODUCTION

During the Extended Observing Period (EOP) of the North American Monsoon Experiment (NAME; Higgins et al. 2005), which took place during the summer of 2004 in northwestern Mexico, observations were made from three radars – the National Center for Atmospheric Research (NCAR) S-Pol polarimetric radar, and two Mexican weather service (SMN) Doppler radars. These three radars formed a network covering a significant portion of the western slope of the Sierra Madre Occidental (SMO) and adjoining coastal plain, the southern half of the Gulf of California, and the southern tip of the Baja California peninsula during much of July and August – in other words, the central location and time period of the North American Monsoon.

Due to difficulties in calibrating the SMN radars and severe blockage by the SMO peaks, a major effort was required to do quality control and correct the data. This involved intercomparison between the SMN radars and the well-calibrated S-Pol radar, and polarimetric-based methodologies to correct beam blockage. The corrected data were then combined into a regional 2-D composites of near-surface rainfall and radar reflectivity, which are being verified against rain estimates from the NAME Event Raingage Network (NERN) as well as estimates from the Tropical Rainfall Measurement Mission (TRMM) satellite.

These composites are available every 15 minutes during the NAME EOP, and provide a useful tool for understanding tropical convective organization and evolution in complex terrain, for verifying satellite estimation of rainfall, and for validating model simulations in this region.

**Corresponding Author Address*: Timothy J. Lang, Dept. of Atmospheric Science, Colorado State Univ., Ft. Collins, CO 80523; e-mail: tlang@atmos.colostate.edu

2. RADAR NETWORK DESCRIPTION

Figure 1 demonstrates the basic geometry of the NAME radar network. The S-Pol radar is an S-band dual-linearly polarized Doppler radar, maintained by the National Center for Atmospheric Research, that has been used in many prior field projects (e.g. TRMM-LBA, MAP, STEPS). S-Pol was deployed during 8 July through 21 August 2004, and was run in two modes.

The first and most common was a climatological mode with low pulse repetition frequency (PRF; 720 Hz or ~210 km range) where the radar scanned a full 360° volume scan in 15 minutes. The second, accounting for about 80 hours of data collection, focused on storm evolution with 2-3 PPI sector volumes and one set of low-angle 360° surveillance scans for rain mapping. Occasionally a few RHI sweeps were included. This storm evolution mode used a PRF of 960 Hz (~150 km range).

The SMN radars are non-polarimetric C-band Doppler radars. The radars were operational prior to NAME, but did not record their data. Guasave was upgraded to temporarily record data on 10 June 2004. Cabo was similarly upgraded on 15 July. Both radars recorded data into the fall, though currently Cabo data post-14 August have not been fully retrieved and processed. Guasave data are processed for 8 July through 21 August. However, due to a disk failure Guasave data are mostly missing during 22 –31 July.

During NAME the SMN radars ran at a single elevation angle and did not do full volumes. For Cabo this angle was 0.6°.

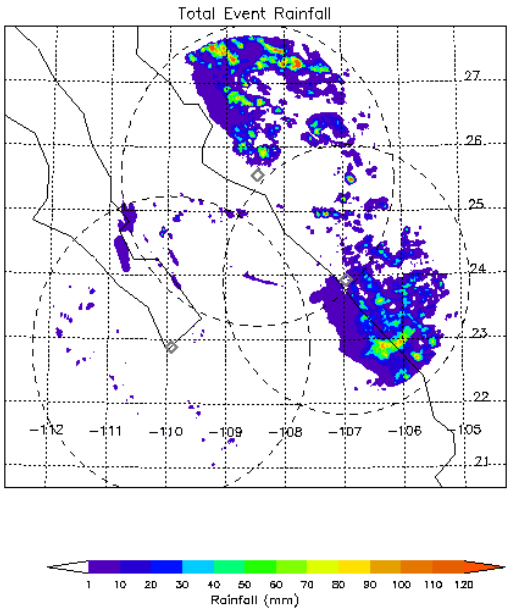

Figure 1. Example rainfall product demonstrating the NAME radar network geometry. Cabo is the westernmost radar, Guasave the northernmost, and S-Pol the easternmost (gray diamonds). Maximum range rings (dashed curves) and lat/lon grid also shown. Product is total rainfall for 17 July 2004.

Guasave varied between 0.5, 1.0, and 1.5° depending on how the visiting engineer or radar operator set the radar during site visits every few days. NAME scientists had limited influence on the scan and PRF settings for the SMN radars, which were driven primarily by engineering and operational constraints. PRF settings often changed every few days, but typically both radars had data coverage out to ~230 km at least.

3. QUALITY CONTROL OF S-POL DATA

S-Pol data were corrected for attenuation as well as clutter, insect, and second-trip contamination. The rainfall attenuation correction methodology was based off Carey et al. (2000). Z_h for all radars (including SMN) was further corrected for gaseous attenuation using established values (Battan 1973). Non-meteorological echo was removed via thresholds on various polarimetric fields, including reflectivity (Z_h), differential reflectivity (Z_{dr}), standard deviation of differential phase (Φ_{dp}). A combination of thresholds on linear depolarization ration (LDR) and Φ_{dp} was used to remove second-trip echo.

Despite all the thresholds, some clutter and insect echo remained after automated filtering. These remaining spurious echoes were subsequently removed by hand with the NCAR soloii software package. In addition, we despeckled the data using the soloii algorithm. This removed any echo that contained only 2 or fewer contiguous gates.

Φ_{dp} was filtered using a 21-gate (3.15-km; 150-m gate spacing) finite impulse response filter developed by V. N. Bringi of Colorado State University. K_{dp} was calculated from the slope of a line fitted to the filtered Φ_{dp} field. The window over which this line was fitted changed depending on the Z_h of the central gate. If Z_h < 35 dBZ, then we fitted to 31 gates (4.65 km). For Z_h between 35 and 45 dBZ, we fitted to 21 gates (3.15 km). For Z_h > 45 dBZ, we fitted to 11 gates (1.65 km).

Significant amounts of beam blockage occurred in S-Pol's northeast sector (351-105° azimuth). This blockage was caused by mountain peaks intercepting the radar beam at low elevation angles. The location of the blocks was determined to the nearest degree in azimuth and nearest km in range by visual inspection of clear-air radar sweeps.

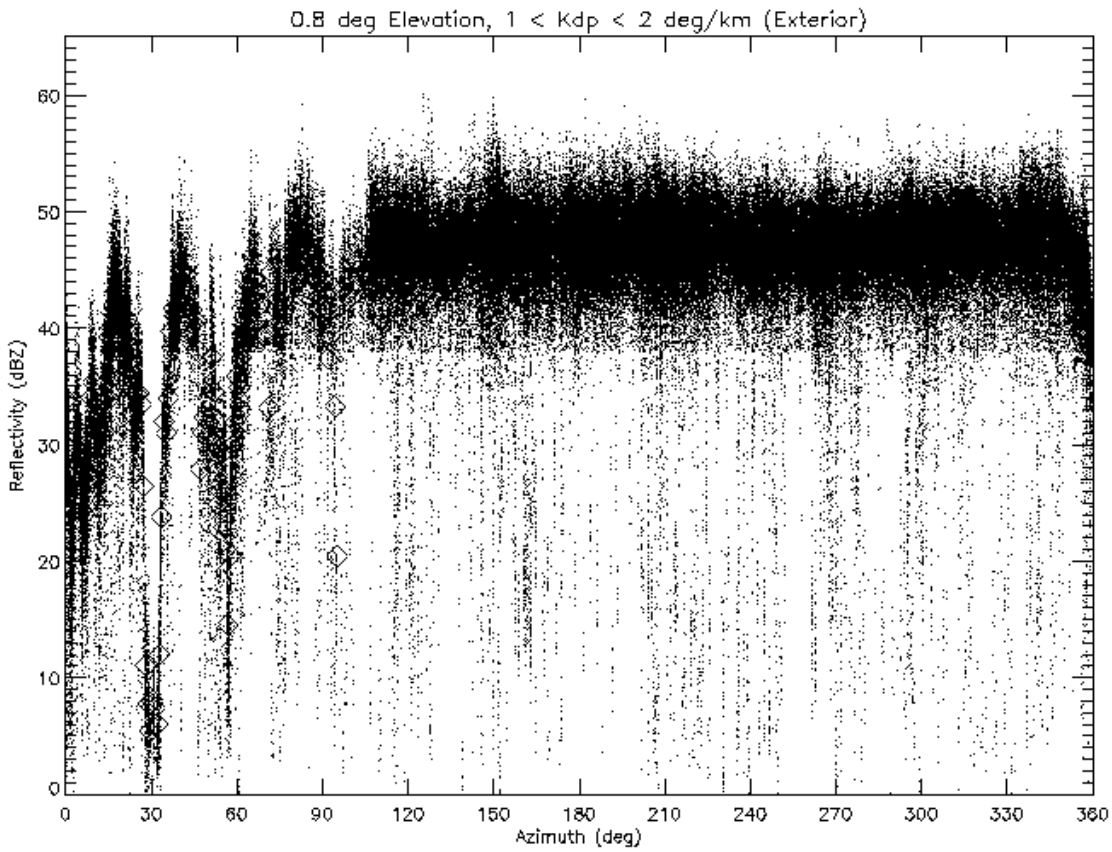

Figure 2. Reflectivity of S-Pol gates (dots) with Kdp between 1 and 2 ° km^{-1}, as a function of azimuth, for 0.8° elevation angle. Data are Version 2 prototype S-Pol data from 8/2-8/9/2004 and include a filter on points with Z_h < 38 dBZ and Φ_{dp} < 15°. Diamonds are median reflectivities at each azimuth.

Then, in the blocked regions, we examined the behavior of Z_h as a function of azimuth for a given range of K_{dp}. Due to the elf-consistency between polarimetric variables (Scarchilli et al. 1996), for a given range of K_{dp}, Z_h should vary only over a small range as well. If Z_h drops significantly below this range, that signals a block. The difference in the median Z_h values in unblocked regions, and median Z_h values in a blocked ray, is the +dBZ correction that needs to be applied to Z_h. Blockage at 0.8° elevation is shown in Fig. 2. Note the significant amounts of blockage in the 351-105° azimuth range.

However, due to scatter in the K_{dp} fields, we decided (for Version 1 data) to use this methodology to only correct small blocks (-2 to -5 dBZ). Larger blocks were not corrected, as when we did they tended to be overcorrected due to the noisy K_{dp} behavior. Instead, we created a composite rain map using input from all three rain map angles (0.8, 1.3, and 1.8° elevation). Where possible, we used rays and gates from 0.8°. If 0.8° had a severe block in a particular ray (reduction > 5 dBZ) then we used information from 1.3° at all ranges greater than that of the block.

If the 1.3° ray itself was severely blocked, then we resorted to 1.8° (which was never blocked more than 5 dBZ). In addition, we filled in low-level gaps caused by clutter removal (0.8° and 1.3°) using information from higher sweeps (1.3° and 1.8°). Quality control (QC) flags reflecting the elevation angle used at a particular gate in the blocked azimuths were created, and are reflected in the height MSL field in the final regional composites. An example of these QC flags, and how the multiple angles were merged to form a single sweep of near-surface data, is shown in Fig. 3.

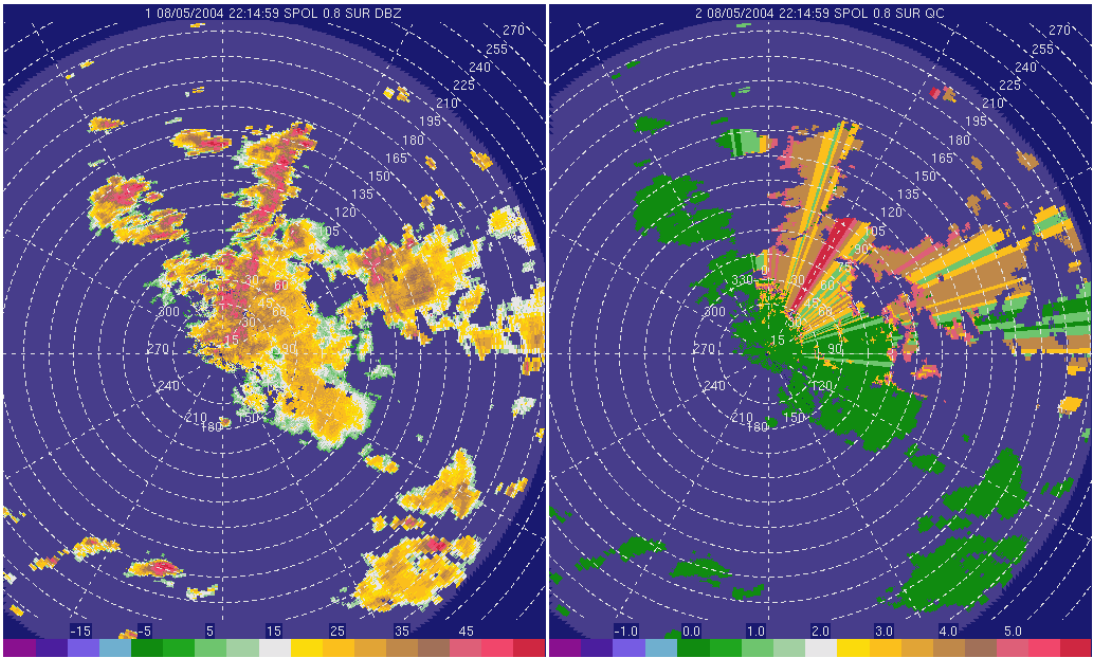

Figure 3. PPIs of reflectivity (left) and QC flags (right) for merged S-Pol data, using 3 elevation angles to correct blockage in the northeastern sector. In the QC field, 0 means unblocked 0.8°; 1 is blockage-corrected 0.8°; 2 is uncorrected 0.8° in a blocked region, but with no 1.3° or 1.8° echo available above the gate; 3 is unblocked 1.3°, 4 is blockage-corrected 1.3°, 5 is unblocked 1.8°, 6 is blockage-corrected 1.8°.

This blockage correction methodology is experimental and requires further analysis and improvements. Version 1 S-Pol data within the 351-105° azimuths is expected to be of inferior quality to the data outside these boundaries. For Version 2, due this fall/winter, we have improved the K_{dp} estimation methodology and reduced noisy behavior in these fields. This allows blockage correction to occur for greater blocks than 5 dBZ, allowing more reliance on data from lower angles in S-Pol's northeastern sector. We still will need to use higher angles than 0.8° for the large block near 30° azimuth, and a couple blocks elsewhere.

Note that for Version 1 we never corrected Z_{dr} within minor blocks, only Z_h. If we corrected blocked Z_h by applying a +dBZ offset, then we set Z_{dr} to a missing data value.

Rain rates were calculated using a modified version of the CSU blended rainfall algorithm (Cifelli et al. 2002). This algorithm varies between $R(K_{dp})$, $R(Z_h,Z_{dr})$, $R(Z_h)$, and $R(K_{dp},Z_{dr})$ depending on the values of the polarimetric variables and the presence of mixed-phase precipitation. It has been demonstrated to provide superior rain estimates to Z-R or any other polarimetric rain estimator alone.

The modifications to this algorithm were as follows:

1) K_{dp}-based rain estimates were not used if K_{dp} did not fall within the expected range of behavior, which depends on the corresponding Z_h value. This occurred even if all other conditions for $R(K_{dp})$ or $R(K_{dp},Z_{dr})$ were met.

2) The Z-R used was $Z=221R^{1.25}$. This was capped at 53 dBZ to avoid hail contamination. Note that, in regions, with significant amounts of mixed-phase

precipitation, usually we were using other polarimetric rain estimators (e.g., $R(K_{dp})$), not a Z-R. This Z-R was determined via intercomparisons of reflectivity with gage rain rates at the NOAA profiler site NW of S-Pol. A mean polarimetrically tuned Z-R via the methodology of Bringi et al. (2004) was determined to be $Z=132.9R^{1.5}$; however, this was not used since it was mainly applicable to heavy convection and not the typical areas where the blended algorithm applied a Z-R (e.g., regions of low Z_h). The Z-R we used is more reflective of a variety of rain situations besides just heavy convection.

3) The maximum rain rate allowed was 231.5 mm/hr, which is the R associated with Z=53 dBZ. If $R > R_{max}$ (no matter what the final method used to estimate R was), then R was set to R_{max}.

4. QUALITY CONTROL OF SMN RADAR DATA

Due to the low PRFs used, we never addressed the quality control of the SMN radar velocity data, only reflectivity. As Cabo and Guasave ran at only one sweep angle, there were updates every minute or so. We only used the most complete sweep closest in time to each 15-minute mark (##:00, ##:15, ##:30, and ##:45). This usually meant the sweep was within 0-2 minutes of this mark. This matched the 15-minute update time of the S-Pol scanning

SMN radar quality control was half-automated, half-not. We applied automated filters on Z_h, Z_h & noise-corrected power (NCP; usually NCP is sufficient alone but the low PRFs required an additional filter on Z_h to avoid deleting turbulent convective cores), and on total power. The value of these filters changed as calibration offsets changed every few days. The specific values were determined by visual inspection of each setting's associated time period. After filtering was performed, we despeckled the data using the same methodology as S-Pol despeckling. These automated procedures removed most of the noise.

Due to antenna backlash, Guasave required a correction to measured azimuths. The correction applied depended on the rotation direction of the antenna (which changed every few days) and the azimuthal spacing of the beams (which changed occasionally when calibration settings changed). The correction varied between +/- 0.42 and 0.63 deg.

We then applied an automated clutter filter to Guasave data. This clutter filter queried a clutter map created from clear-air Guasave sweeps taken over several days. Due to different PRFs, elevation angles, and pulse lengths, we had separate clutter maps for July and for August Guasave data. For each gate in every ray, we queried the clutter map to see if clutter occupied that position. If so, the data were removed.

We hand edited the filtered datasets for any remaining clutter, noise, second-trip, and insects using soloii. Cabo data did not have many storms overrun its clutter, so its clutter was hand edited out using soloii, and no automated filter was used.

A reflectivity offset was then applied to the data based on visual and statistical intercomparisons with S-Pol reflectivities. The statistical evaluation compared the closest gates within 500 m horizontal and 200 m vertical. Histograms of reflectivity differences were obtained from this statistical intercomparison. In addition, visual intercomparison of well-placed echoes was done using soloii. Based on both these methods, a reflectivity correction was applied to the SMN radar data. The value of this correction depended on the particular setting of Guasave, which varied throughout the NAME EOP. Typically, several days would pass and a new setting occurred, as discussed before. No gradual drift in calibration was observed, only step-wise changes. This was confirmed by examining time series of noise reflectivity at a specific range. Occasionally, a calibration change lasted only a few hours, or even only one sweep. These often did not lend themselves well to intercomparison with S-Pol, due to the meteorological situation. Under these circumstances, visual and statistical intercomparisons were made with SMN radar sweeps immediately prior to and after the time of the "rogue" setting. In addition, we examined noise reflectivity to identify rogue settings that were similar in terms of offset.

Attenuation correction by rain was based on the GATE project algorithm (Patterson et al. 1979), which uses a Z-R to estimate rainfall, then iteratively corrects Z

at a gate based on the theoretical treatment of attenuation by all the rainfall up to the given gate. The Z-R used was the same as the S-Pol Z-R, $Z=221R^{1.25}$. The typical C-band correction is usually on the order of +2-3 dBZ downrange of significant convection.

The values of the final applied Z_h offset for Guasave varied from +6 dBZ to -7 dBZ, depending on the particular setting. Final Z_h offsets for Cabo varied between 0 and +6 dBZ. The attenuation-corrected SMN data were intercompared with the attenuation-corrected S-Pol data to confirm all the applied offsets. We believe that final, corrected SMN Z_h measurements are accurate to within 1-2 dBZ.

Guasave did not appear to have many blocks. However, at low angles in July, Z_h values near 25° azimuth were partially blocked, but no correction for blockage was attempted. Cabo was partially blocked by terrain between 300° and 60° azimuth. However, most storms remained outside this region. No blockage correction was attempted here either.

SMN radar rainfall rates were determined from the aforementioned Z-R relationship, with capping at 53 dBZ (231.5 mm/hr) to avoid hail contamination.

5. REGIONAL COMPOSITE CREATION

The Version 1 regional composites were created on 3 different latitude/longitude grid spacings – 0.01°, 0.02°, and 0.05° (~1, 2, and 5 km). The files, available every 15 minutes during the NAME EOP, contain near-surface reflectivity, near-surface rain rate, and mean height (m MSL) of the radar beams used at each grid point. This latter field allows the user to decide whether or not to use the data (for example, rain rates when the actual radar beam is above freezing level). This is especially important for data at long ranges from a radar, and also S-Pol data that underwent blockage correction. Separate missing data flags are used when a radar was missing from the composite, or if the radar was present but no echo was detected.

Sweeps from about the same time and the lowest elevation angle were combined every 15 minutes to produce network composites. Before converting to a latitude/longitude grid, the data along each ray were smoothed and resampled to a more sparse array. Logarithmic fields (i.e., Z_h) were linearized first. The moving average window applied along the range dimension was approximately 1000 m long.

Where radar gates from different radars overlapped, the lowest gate took precedence and higher gates were eliminated. Note that this did not necessarily preserve the highest reflectivity gate in a vertical column. However, since reflectivity usually decreases with height, this was generally the case. Future versions of the composite dataset may include such a field based on the highest reflectivity found in a vertical column, but there are not expected to be large differences. An overlap occurred wherever a gate from one radar was within one half-gate width and one half-beam width of a gate from another radar.

After eliminating higher gates from overlapping sections, the remaining gates were combined and interpolated to a regular lat/lon grid. An inverse-distance weighting method was employed to produce the interpolated values using only gates within 0.03° of each gridpoint. A circular smoothing filter with a radius of 0.001° was also applied.

6. FUTURE PLANS

For Version 2 data, due this fall/winter, we plan the following changes:

1) We will improve S-Pol filtering to provide better estimates of K_{dp} and better removal of clutter, insects, etc. Work on this is finished, and the results show vast improvements over Version 1, particularly with respect to smoother and less noisy K_{dp} fields.

2) We will revisit the S-Pol blockage correction methodology, and attempt to improve upon it. Work on this has begun, and with the smoother K_{dp} fields from Version 1, the results appear to be much better. This means less reliance on upper angles and better correction of the base 0.8° scan. The end result will be a smoother, more accurate rainfall field in the blockage region.

3) We will examine the performance of our Z-R relationship, and make

improvements where necessary. This could involve stratiform/convective partitioning and use of a polarimetrically tuned Z-R.

4) We will examine the performance of the SMN radar attenuation correction methodology, and make improvements where necessary. This will depend on the development of a more accurate Z-R set.

5) We will correct any errors made in the hand editing of SMN and S-Pol radar data.

6) Where possible, we will provide error statistics on the rain rate estimates.

7) We will refine the estimates of Z_h biases in the SMN radar data using intercomparisons with TRMM overpasses during NAME. Preliminary results here suggest that the bias correction is working properly. However, attenuation behind significant convective cores may be underestimated, requiring improvements to the SMN radar attenuation scheme.

8) We will fill in existing radar and time gaps where data are available.

7. DISCUSSION AND CONCLUSIONS

This paper has discussed the quality control of radar data from the NAME project, and the development of 2-D regional grids of near-surface rainfall and reflectivity. These regional composites of the three NAME radars will be used to study convective development and organization, as well as the diurnal cycle of precipitation in this region. We will also study the relationship between large-scale forcing and convection in this region. These results will be used to help motivate and provide context for case studies of particular events. Examples of these research thrusts will be shown in Part 2 of this study (Lang et al. 2005).

8. ACKNOWLEDGMENTS

We thank Jon Lutz and Bob Rilling of NCAR, Arturo Valdez-Manzanillo of the University of Tabasco, and Armando Rodriguez of SMN, as well as other NCAR S-Pol and SMN radar staff, for their help with data collection and quality control. This work was funded by NSF grant ATM-0340544 and NOAA grant NA17RJ1228.

9. REFERENCES

Battan, L. J., 1973: *Radar Observation of the Atmosphere*, University of Chicago Press, 324 pp.

Bringi, V. N., T. Tang, and V. Chandrasekar, 2004: Evaluation of a new polarimetrically based Z–R relation. *J. Atmos. Ocean. Technol.*, **21**, 612–623.

Carey, L. D., S. A. Rutledge, D. A. Ahijevych, and T. D. Keenan, 2000: Correcting propagation effects in C-Band polarimetric radar observations of tropical convection using differential propagation phase. *J. Appl. Meteorol.*, **39**, 1405–1433.

Cifelli, R., W. A. Petersen, L. D. Carey, and S. A. Rutledge, 2002: Radar observations of the kinematic, microphysical, and precipitation characteristics of two MCSs in TRMM-LBA. *J. Geophys. Res.*, **29**, 10.1029/2000JD0000264.

Higgins, W., et al., 2005: The North American Monsoon Experiment (NAME) 2004 field campaign and modeling strategy. Submitted to *Bull. Amer. Meteorol. Soc.*

Lang, T. J., R. Cifelli, D. Lerach, L. Nelson, S. W. Nesbitt, G. Pereira, S. A. Rutledge, D. Ahijevych, and R. Carbone, 2005: Radar observations during NAME 2004. Part II: Preliminary results. *32nd Conf. on Radar Meteorol.*, Amer. Meteorol. Soc., Albuquerque, NM.

Patterson, V. L., M. D. Hudlow, P. J. Pytlowany, F. P. Richards, and J. D. Hoff, 1979: GATE radar rainfall processing system. NOAA Tech. Memo. EDIS 26, NOAA, Washington, DC, 34 pp. [Available from National Technical Information Service, Sills Building, 5285 Port Royal Road, Springfield, VA 22161.].

Scarchilli, G., E. Gorgucci, V. Chandrasekar, and A. Dobaie, 1996: Self-consistency of polarization diversity measurement of rainfall. *IEEE Trans. Geosci. Remote Sens.*, 34, 22-26.